Mid-Infrared Imaging of Massive Star Formation in Cygnus-X

Joseph L. Hora[1], H. A. Smith[1], R. L. Doering[2], R. A. Gutermuth[3], K. E. Kraemer[4], X. Koenig[5], S. Bontemps[6], S. T. Megeath[7], N. Schneider[8], F. Motte[8], S. Carey[9], R. Simon[10], E. Keto[1], L. E. Allen[11], G. G. Fazio[1], S. Price[4], D. Mizuno[4], J. D. Adams[12]

[1]Harvard-Smithsonian Center for Astrophysics, [2]University of Wisconsin-Madison, [3]Smith College, [4]Air Force Research Laboratory, [5]NASA/GSFC, [6]Observatoire de Bordeaux,[7]Univ. of Toledo, [8]CEA-Saclay, [9]Spitzer Science Center, [10]Universität zu Köln, [11]NOAO, [12]Cornell University

Abstract

Cygnus–X is the richest known concentration of massive protostars and the large OB associations within 2 kpc and a unique laboratory to study the earliest stages of massive star formation. Previously, with the IRAC and MIPS infrared cameras (Fazio et al. 2004, Rieke et al. 2004) on the Spitzer Space Telescope, we conducted an unbiased survey of 24 square degrees of the Cygnus-X region (Hora et al. 2009). The sample includes protostars and young stars with a range of masses and at various stages of evolution.

To better resolve the more complex regions and measure fluxes of sources bright enough to saturate the Spitzer cameras, we conducted a follow-up survey with NASA's Infrared Telescope Facility (IRTF). We present the initial results from our IRTF survey here. The IRTF has an angular resolution about 3 times better than Spitzer and the MIRSI camera does not saturate at the flux levels of sources in Cygnus-X. Although our Spitzer observations have much higher sensitivity, our IRTF observations of the brighter, more complex regions better resolve multiple sources and better determine the distribution of fluxes between the various protostars and the emission from the ISM.

The IRTF images, along with the Spitzer images and IRS spectra, will enable us to determine the properties of the young massive stars in Cygnus-X and to examine their effects on the surrounding ISM including the possible triggering of further generations of star formation.

Observations and Reduction

We chose regions for our follow-up IRTF survey by searching our Cygnus-X survey for regions that appear saturated, marginally resolved, or composed of multiple sources. For the IRAC data taken in 12s HDR mode, the saturation level at 8 μm was about 2.5 Jy. For MIPS in the fast scanning mode at 24 microns the saturation level was about 4 Jy. A total of 54 positions were identified.

The new data were obtained at the IRTF in two separate observing runs in July 2009 and July-August 2010. We used the 90x60 arcsec imaging mode of MIRSI (Kassis et al. 2008), the 8.7, 11.6 and 24.4 μm filters (with bandpasses of 8.9, 9.9, and 7.9%, respectively), and the standard mid-IR techniques of secondary chopping and telescope nodding. For compact sources, chop and nod throws of ~30 arcsec were used, with all beams on the detector to maximize sensitivity and efficiency. For extended objects, the beam switch size was increased to chop and nod completely off the object. Infrared standard stars such as β Peg, α Tau, and β And were used for flux standards to calibrate the observations. MIRSI's 5σ sensitivity in one minute of on-source time is approximately 74, 110, and 1060 mJy at 8.7, 11.6, and 24.4 μm, respectively. The integration times ranged from about 1 minute for bright sources to 20 minutes for the faintest sources observed.

The data were reduced using a set of IRAF scripts written for MIRSI. First, the chop/nod frames were subtracted to remove sky and instrument backgrounds. Then the pattern noise that is common to all MIRSI output channels (Kassis et al. 2008) was removed by a median-filtering technique. Any offset present in the output channels was then subtracted, and a "flat field" or pixel gain correction was applied. The gain images were derived from observations of the observatory dome flat field screen and sky using the same telescope orientation. Noisy and low responsivity pixels were flagged and not used in the construction of the mosaics.

References

Fazio, G. G. et al., 2004, ApJS, 154, 10
Furuya et al. 2000, ApJL, 542, L135
Gehrz, R. et al. 1982, 254, 550
Gutermuth, R. et al. 2008, ApJ, 674, 336
Hora, J. L. et al. 2009, AAS, 41, 498
Kassis et al. 2008, PASP, 120, 127
Rieke, G. H. et al. 2004, ApJS, 154, 25
Robitaille, T. P. et al. 2007, ApJS, 169, 328
Sridharan, T. K. et al., 2002, ApJ, 556, 931

Acknowledgments

This work is in part based on observations made with the Spitzer Space Telescope, operated by JPL/Caltech under NASA contract 1407. Support for this work was provided by NASA through Contract #1256790 issued by JPL/Caltech.

IRAS 20319+3958

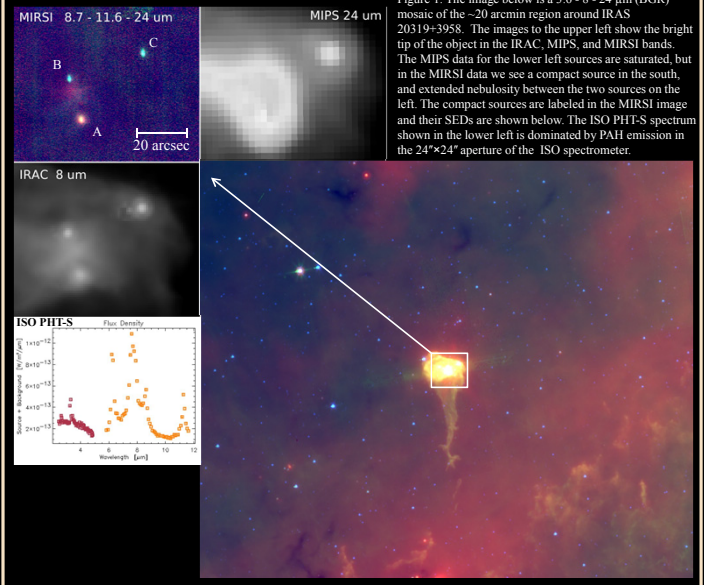

Figure 1. The image below is a 3.6 - 8 - 24 μm (BGR) mosaic of the ~20 arcmin region around IRAS 20319+3958. The images to the upper left show the bright tip of the object in the IRAC, MIPS, and MIRSI bands. The MIPS data for the lower left sources are saturated, but in the MIRSI data we see a compact source in the south, and extended nebulosity between the two sources on the left. The compact sources are labeled in the MIRSI image and their SEDs are shown below. The ISO PHT-S spectrum shown in the lower left is dominated by PAH emission in the 24"×24" aperture of the ISO spectrometer.

The infrared source IRAS 20319+3938 was identified as a High Mass Protostellar Object (HMPO) by Sridharan et al. (2002). The Spitzer image in Figure 1 above shows it as the bright tip of a "tadpole"-shaped structure with an elliptical head consisting of 3 compact sources embedded in bright nebulosity and a tail pointing away from the massive Cyg OB2 association to the north. The bright nebulosity is dominated by PAH emission (see ISO spectrum above) that is excited either internally by the 3 compact sources and/or externally by the Cyg OB2 association. The tail appears to be material streaming away from the head, driven by outflow and radiation from Cyg OB2.

The ISO spectrometer's beam was too large to separate the compact and extended emission in this source. With the MIRSI and Spitzer observations, we can examine the Spectral Energy Distributions (SEDs) of the compact sources and determine their individual properties. Figure 2 below show the SEDs for the three compact objects, combining 2MASS, Spitzer, and MIRSI photometry. Source A is seen to be quite distinct from sources B and C, dominating the 24 μm emission from the region. This can be seen in the color image above where source A appears much redder than the other two sources. There is extended nebulosity near source B which causes it to saturate the MIPS image, but in the MIRSI data we can separate this from the compact source to accurately determine its SED. Sources B and C are very similar, except that source C has higher emission at 12 and 24 μm. On the basis of their near-IR and Spitzer fluxes, sources B and C are determined to be Class II young stellar objects, using the methods of Gutermuth et al. (2008).

None of the compact sources show evidence of strong PAH emission at 7.7 μm, suggesting that the emission seen in the ISO spectrum is predominantly in the surrounding nebulosity.

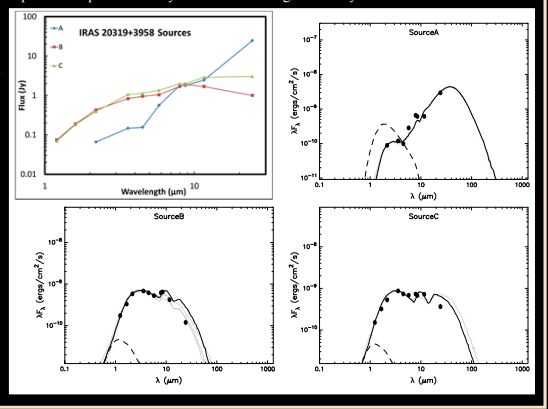

Figure 2. Top Left: The SEDs of the three compact sources detected in IRAS 20319+3958. The points at 1.2, 1.6, and 2.2 μm are from 2MASS, the 3.6, 4.5, 5.8 and 8.0 μm points are the IRAC data, and the 8.7, 11.6, and 24.4 μm points are the MIRSI data. The MIRSI and IRAC fluxes agree well where they overlap near 8 μm. Top Right, Bottom: results from the SED model fitter of Robitaille et al. (2007). Source A is fit by models of approximately the same stellar mass (~7 M) as sources B and C, but the best fitting models for Source A are much younger (~10^5 yr) in comparison to Sources B and C (~10^6 yr).

DR 21 Region

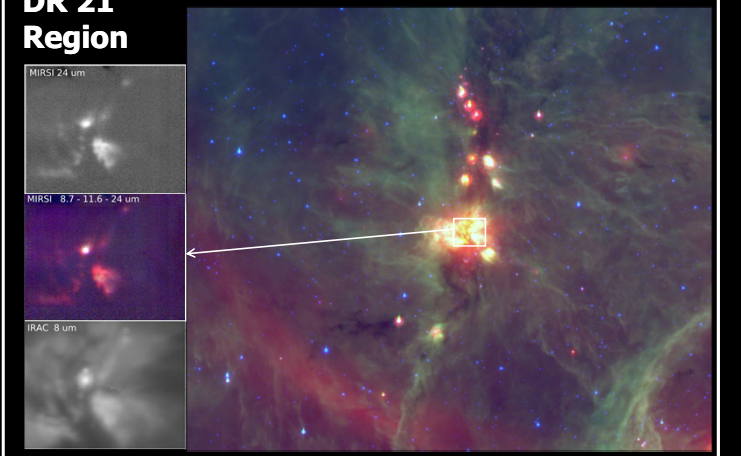

Figure 3. The image above right is a 3.6 – 8 – 24 μm (BGR) mosaic of the ~20 arcmin region around DR 21. The images to the left show the bright tip of the object in the IRAC and MIRSI bands. The entire small region is saturated in the MIPS image (not shown separately) .

DR 21 contains one of the most massive star formation regions and molecular outflows in our galaxy. The extended DR 21 nebula consists of a filamentary ridge of massive star-forming clusters that stretch from DR 21 (main), seen in the center of Figure 3, northward to W75N, and includes clusters around the bright maser source DR 21(OH). Along with the rest of the Cygnus-X complex in which it is embedded, DR 21 appears as part of a shell-like structure around the supermassive Cyg OB2 association.

The IRAC 4.5 μm image traces the shocked molecular hydrogen emission in the outflow region (Smith et al. 2006). The core is dominated by emission from a bright compact source near the dark line of the 8 μm image, which is also bright at 24 μm in the MIRSI image. However, a significant amount of the total flux in the region is emitted by the extended nebulosity which surrounds the core near the origin of the outflows.

S 106

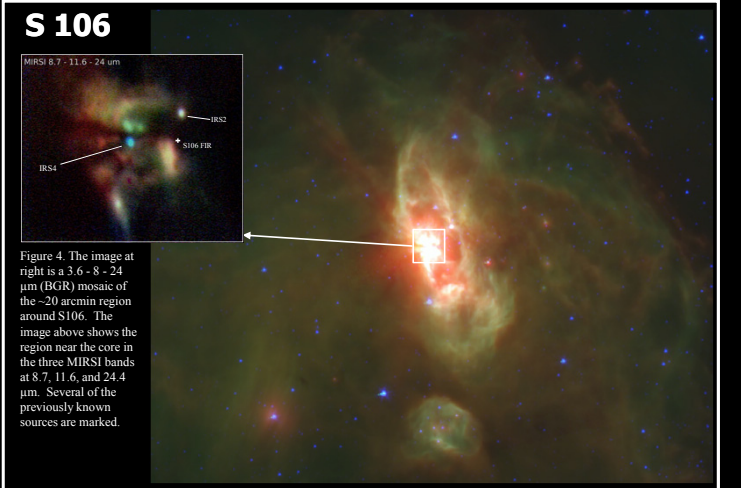

Figure 4. The image at right is a 3.6 - 8 - 24 μm (BGR) mosaic of the ~20 arcmin region around S106. The image above shows the region near the core in the three MIRSI bands at 8.7, 11.6, and 24.4 μm. Several of the previously known sources are marked.

S106 is a star-forming region with a bipolar outflow morphology. It is dominated by an O7-O9 star in its core (IRS4; Gehrz et al. 1982) which illuminates the surrounding molecular cloud. The Spitzer image in Figure 4 shows the larger molecular cloud in which this young star is embedded. The MIRSI image shows a number of compact sources and the structure of the nebulosity surrounding the exciting sources in the core of S106. The cross shows the location of the water masers near the class 0 source S106 FIR (Furuya et al. 2000).

Poster 258.07 2011 January 9-13 217TH AAS meeting Seattle, WA